Translation initiation or elongation inhibition triggers contrasting effects on *Caenorhabditis elegans* survival during pathogen infection

Annesha Ghosh[1] and Jogender Singh[1,*]

[1]Department of Biological Sciences, Indian Institute of Science Education and Research, Mohali, Punjab, 140306, India

[*]For correspondence: jogender@iisermohali.ac.in

Keywords: innate immunity, lifespan, *P. aeruginosa*, translation, ZIP-2

Abstract

Diverse microbial pathogens are known to attenuate host protein synthesis. Consequently, the host mounts a defense response against protein translation inhibition, leading to increased transcript levels of immune genes. The seemingly paradoxical upregulation of immune gene transcripts in response to blocked protein synthesis suggests that the defense mechanism against translation inhibition may not universally benefit host survival. However, a comprehensive assessment of host survival on pathogens upon blockage of different stages of protein synthesis is currently lacking. Here, we investigate the impact of knockdown of various translation initiation and elongation factors on the survival of *Caenorhabditis elegans* exposed to *Pseudomonas aeruginosa*. Intriguingly, we observe contrasting effects on *C. elegans* survival during *P. aeruginosa* exposure upon inhibition of initiation and elongation factors. While inhibiting both initiation and elongation factors leads to an upregulation of immune gene expression and reduced colonization of the *C. elegans* gut by *P. aeruginosa*, inhibiting initiation factors proves beneficial, whereas inhibiting elongation factors proves detrimental to *C. elegans* survival. We demonstrate that the bZIP transcription factor, ZIP-2, mediates both the advantageous and deleterious effects of inhibiting translation initiation and elongation. Therefore, our findings unveil the opposing roles of translation initiation and elongation in *C. elegans* survival during *P. aeruginosa* infection, with the same transcription factor, ZIP-2, orchestrating these opposing effects.

Introduction

Eukaryotic mRNA translation is a highly regulated and energy-consuming process involved in synthesizing proteins from mRNAs (Jackson et al. 2010; Buttgereit & Brandt 1995). The translation mechanism is critically governed by a combination of initiation, elongation, and release factor polypeptides (Gebauer & Hentze 2004). Beyond its role in protein synthesis, translation regulates various biological functions such as proteostasis, integrated stress response, neuronal activity, germline apoptosis, and lifespan (Curran & Ruvkun 2007; Gonskikh & Polacek 2017; Clay et al. 2023; Hansen et al. 2007a; Pan et al. 2007; Contreras et al. 2008; Blazie et al. 2021; Starck et al. 2016). Different stresses, such as heat shock, nutrient stress, hypoxia, and DNA damage, lead to a general shutdown and reprogramming of translation (Spriggs et al. 2010; Singh 2020). The integrated stress response triggered by diverse stress signals converges on the global attenuation of translation (Pakos-Zebrucka et al. 2016). A reduced translation rate is essential for survival under stressful conditions (Howard et al. 2016; Hansen et al. 2007a; Rogers et al. 2011), and both translation rate and fidelity play a crucial role in regulating lifespan across various species. Enhanced fidelity of protein synthesis has been linked to increased lifespan (Xie et al. 2019; Martinez-Miguel et al. 2021). Likewise, a reduction in translation rates in otherwise healthy organisms results in an extended lifespan (Hansen et al. 2007a; Pan et al. 2007).

A multitude of polypeptide factors regulate translation initiation and elongation steps (Gebauer & Hentze 2004; Jackson et al. 2010). Inhibition of translation initiation or elongation can result in different physiological responses (Knight et al. 2020; Clay et al. 2023). For example, inhibiting translation initiation protects against heat and age-associated protein aggregation but does not shield against proteotoxicity caused by proteasome dysfunction. Conversely, inhibiting translation elongation protects against heat and proteasome dysfunction but does not guard against age-associated protein aggregation (Clay et al. 2023). Interestingly, inhibiting both translation initiation and elongation increases the lifespan of the roundworm *Caenorhabditis elegans* (Li et al. 2011; Statzer et al. 2022). Therefore, understanding the role of different translation stages in various physiological processes is important.

Several microbial toxins block host translation (Remick et al. 2023; Mohr & Sonenberg 2012), prompting organisms to evolve mechanisms that sense perturbations in protein translation and activate immune responses (Chakrabarti et al. 2012; Fontana et al. 2011; Mohr & Sonenberg 2012). In *C. elegans*, translation inhibition by the bacterial pathogen *Pseudomonas aeruginosa* results in the increased expression of immune genes

(Dunbar et al. 2012; McEwan et al. 2012; Govindan et al. 2015). Even in the absence of the pathogen, translation inhibition results in the activation of immune and xenobiotic responses (Dunbar et al. 2012; Govindan et al. 2015; McEwan et al. 2012; Melo & Ruvkun 2012). Lipid signaling-regulated MAP kinases and the bZIP transcription factor ZIP-2 are known to regulate the surveillance immunity activated by translation inhibition (Govindan et al. 2015; Dunbar et al. 2012). Notably, ZIP-2-mediated immune response activation is triggered only by inhibition of translation elongation, not initiation (Dunbar et al. 2012). While the activation of the immune response at the mRNA levels has been monitored, the effects of translation inhibition on the survival of the host against pathogens have not been studied. Increased mRNA levels of immunity genes upon translation inhibition may not necessarily lead to increased production of their polypeptides due to blocked protein synthesis. Thus, a comprehensive analysis of host survival on pathogens upon inhibition of different translation stages is warranted.

In this study, we conducted a comprehensive analysis of the effects of knockdown of different translation initiation and elongation factors on the survival of *C. elegans* on *P. aeruginosa*. Interestingly, we observed that while inhibiting initiation factors either improved or did not change survival, inhibiting elongation factors reduced the survival of *C. elegans* on *P. aeruginosa*. Inhibition of initiation factors increased the expression of immune genes and reduced colonization of the *C. elegans* gut with *P. aeruginosa*. These effects on immune gene expression, reduced colonization, and improved survival were all regulated by the bZIP transcription factor ZIP-2 upon inhibition of translation initiation. Surprisingly, despite resulting in a reduced survival on *P. aeruginosa*, inhibition of translation elongation also led to increased expression of immune genes and reduced gut colonization with *P. aeruginosa*. The decreased survival upon inhibition of translation elongation was also mediated by ZIP-2. Thus, our studies unraveled opposing roles for translation initiation and elongation in the survival of *C. elegans* on *P. aeruginosa* and demonstrated that the same transcription factor, ZIP-2, mediates these contrasting effects.

Results

Inhibition of translation initiation or elongation leads to opposing outcomes on *C. elegans* survival during *P. aeruginosa* infection

Previous studies have demonstrated that the inhibition of translation can impact the germline and development of various organisms (Long et al. 2002; Johnstone & Lasko 2004; Liu et al. 2007; Contreras et al. 2008; Cattie et al. 2016). Therefore, before investigating the impact of

inhibiting different translation factors on *C. elegans* survival on a pathogen, we first elucidated how their inhibition affected the fertility and development of *C. elegans*. We systematically knocked down the 47 initiation and elongation factors available in the Ahringer RNA interference (RNAi) library. Among the 47 translation factors tested, the knockdown of 3 resulted in sterility, while the knockdown of 23 slowed the development of *C. elegans* (Table S1). Because sterility modulates survival on pathogens (Miyata et al. 2008), the translation factors whose knockdown led to sterility were excluded from further analysis. For subsequent experiments, we transferred the worms to RNAi plates after the L3 stage for those translation factors whose knockdown slowed the development.

Next, we studied how the knockdown of different translation factors affected the survival of *C. elegans* on *P. aeruginosa* PA14. We observed that the knockdown of different translation factors resulted in an improved (Figure 1A, 1B), unaltered (Figure 1C, 1D), or reduced (Figure 1E, 1F) survival of *C. elegans* compared to the empty vector control on *P. aeruginosa* (Figures S1 and S2, and Table S2). Intriguingly, while the knockdown of translation initiation factors resulted in either increased or unaltered survival, the knockdown of translation elongation factors resulted in reduced survival of *C. elegans* on *P. aeruginosa* (Figure 1G and Figures S1 and S2, and Table S2). Thus, these studies demonstrated that the inhibition of translation initiation or elongation led to opposing outcomes on *C. elegans* survival during *P. aeruginosa* infection.

Blocking translation initiation enhances *C. elegans* survival on *P. aeruginosa* via the transcription factor ZIP-2

To unravel the immunity pathways contributing to the improved survival of *C. elegans* on *P. aeruginosa* following the inhibition of translation initiation factors, we examined the survival of mutants representing different innate immune pathways. Inhibition of the representative translation initiation factors, *eif-2α* (ortholog of human EIF2S1, eukaryotic translation initiation factor 2 subunit alpha) and *ifg-1* (ortholog of human EIF4G3, eukaryotic translation initiation factor 4 gamma 3), in mutants of various innate immune pathways, including the NSY-1/SEK-1/PMK-1 (Kim et al. 2002), the TGF-β/DBL-1 (Mallo et al. 2002), and the nuclear hormone receptor NHR-8 (Otarigho & Aballay 2020; Peterson et al. 2022), resulted in enhanced survival compared to control RNAi (Figure 2A-2E and Figure S3A-S3E). However, the mutants of the bZIP transcription factor ZIP-2 (Estes et al. 2010) did not exhibit increased survival on *P. aeruginosa* upon the knockdown of *eif-2α* and *ifg-1* (Figure

2F and Figure S3F), suggesting that the enhanced survival upon inhibiting translation initiation factors is mediated by ZIP-2.

Since the knockdown of *eif-2α* and *ifg-1* did not show a significant difference in the survival rate of *zip-2(tm4248)* animals on *P. aeruginosa* compared to control RNAi animals, there is a possibility that *zip-2(tm4248)* animals are RNAi defective. To explore this possibility, we knocked down *act-5* and *bli-3* genes in N2 wild-type, *zip-2(tm4248)*, and RNAi-defective mutant *sid-1(qt9)*. The knockdown of *act-5* and *bli-3* is known to result in development arrest and a blistered cuticle, respectively (Whangbo et al. 2017; Simmer et al. 2003). We observed that N2 and *zip-2(tm4248)* animals were arrested at the L1 stage upon *act-5* RNAi and developed multiple blisters across the larval body upon *bli-3* RNAi (Figure S4). In contrast, the RNAi-defective *sid-1(qt9)* animals did not display these phenotypes and developed into healthy adults on *act-5* and *bli-3* RNAi (Figure S4). These results indicated that *zip-2(tm4248)* animals are not RNAi defective, and the enhanced survival on *P. aeruginosa* upon inhibiting translation initiation factors is likely mediated by ZIP-2.

Inhibition of translation initiation reduces *C. elegans* intestinal colonization with *P. aeruginosa* by activating immune response genes via ZIP-2

Previous studies have shown that the inhibition of translation initiation and elongation results in the increased expression of innate immune and xenobiotic response genes (Dunbar et al. 2012; Govindan et al. 2015). The induction of immunity genes was found to be ZIP-2 dependent upon the inhibition of translation elongation. However, the induction of immunity genes upon the inhibition of translation initiation was considered ZIP-2 independent (Dunbar et al. 2012). Given that enhanced survival on *P. aeruginosa* upon the inhibition of translation initiation was entirely dependent on ZIP-2, we hypothesized that inhibiting translation initiation might trigger ZIP-2-dependent immune responses. We examined the expression of several immune response genes induced by *P. aeruginosa* in a ZIP-2-dependent manner (Estes et al. 2010). Most of the tested genes were significantly induced by the knockdown of *eif-2α* and *ifg-1* in N2 animals (Figure 3A). The induction levels for several of these genes were notably higher with *eif-2α* knockdown compared to *ifg-1* knockdown (Figure 3A). The expression levels of all of these genes declined substantially in *zip-2(tm4248)* animals upon knockdown of *eif-2α* and *ifg*-1, suggesting that the induction of these genes was ZIP-2 dependent (Figure 3B). These results suggested that the inhibition of translation initiation activates a ZIP-2-dependent immune response, contributing to the enhanced survival of animals on *P. aeruginosa*.

The colonization of the gut with *P. aeruginosa* plays a pivotal role in infection and the survival of *C. elegans* under slow-killing conditions (Tan et al. 1999; Das et al. 2023). We investigated whether the inhibition of the translation initiation factors affected the colonization of *C. elegans* gut with *P. aeruginosa*. Knockdown of *eif-2α* and *ifg-1* in N2 animals resulted in a significant reduction in gut colonization by *P. aeruginosa* (Figure 3C, 3D). Subsequently, we evaluated the impact of *eif-2α* and *ifg-1* knockdown on *P. aeruginosa* colonization in different immunity mutants. Inhibition of *eif-2α* and *ifg-1* also resulted in reduced *P. aeruginosa* colonization in *sek-1(km4)*, *pmk-1(km25)*, *dbl-1(nk3)*, and *nhr-8(ok186)* animals (Figure S5). On the other hand, the knockdown of *eif-2α* and *ifg-1* did not result in a significant reduction in *P. aeruginosa* colonization in *zip-2(tm4248)* animals (Figure 3E, 3F). Collectively, these results suggested that inhibition of translation initiation reduced pathogen colonization in *C. elegans* via ZIP-2, thereby enhancing animal survival on *P. aeruginosa*.

ZIP-2 diminishes gut colonization by *P. aeruginosa* upon the inhibition of translation elongation

Next, we sought to understand how the inhibition of translation elongation led to the reduced survival of *C. elegans* on *P. aeruginosa*. We investigated whether inhibiting translation elongation would result in an increased colonization of the gut by *P. aeruginosa*. The knockdown of representative elongation factors, *eft-2* (an ortholog of human EEF2, eukaryotic elongation factor 2) and *eef-1B.2* (an ortholog of human EEF1B2, eukaryotic elongation factor 1 beta 2), significantly reduced gut colonization with *P. aeruginosa* in N2 animals (Figure 4A, 4B). This observation was paradoxical as the knockdown of *eft-2* and *eef-1B.2* reduced the survival of N2 animals on *P. aeruginosa* despite the concurrent reduction in gut colonization by the pathogen.

We evaluated whether any of the immunity pathways mediated the reduced colonization of the gut with *P. aeruginosa* upon the knockdown of *eft-2* and *eef-1B.2*. Inhibition of *eft-2* and *eef-1B.2* resulted in diminished *P. aeruginosa* colonization in *sek-1(km4)*, *pmk-1(km25)*, *dbl-1(nk3)*, and *nhr-8(ok186)* animals (Figure 4C-4J). On the other hand, the knockdown of *eft-2* and *eef-1B.2* did not lead to a significant reduction in *P. aeruginosa* colonization in *zip-2(tm4248)* animals (Figure 4K, 4L), suggesting that the inhibition of translation elongation reduced pathogen colonization in a ZIP-2-dependent manner. Together, these results indicated that the inhibition of translation elongation reduced

the survival of *C. elegans* on *P. aeruginosa*, notwithstanding the decreased colonization of the gut by the bacterium.

Inhibition of translation elongation diminishes *C. elegans* survival on *P. aeruginosa* via ZIP-2

Because the knockdown of elongation factors, *eft-2* and *eef-1B.2*, resulted in reduced colonization by *P. aeruginosa*, we asked whether the inhibition of translation elongation increased the expression levels of immune response genes. A majority of the tested genes exhibited significant induction upon the knockdown of *eft-2* and *eef-1B.2* in N2 animals (Figure 5A). The induction levels for most of these genes were higher in the case of *eft-2* knockdown compared to *eef-1B.2* knockdown (Figure 5A). Intriguingly, the reduction in survival on *P. aeruginosa* was more pronounced upon the knockdown of *eft-2* than *eef-1B.2* (Figure 1G), suggesting that the diminished survival might be attributed to the activation of the immune response. The induction of all of these genes was ZIP-2 dependent, as they were not induced in *zip-2(tm4248)* animals upon the knockdown of *eft-2* and *eef-1B.2* (Figure 5B).

Considering that the inhibition of translation elongation resulted in the activation of a ZIP-2-dependent immune response, we investigated whether ZIP-2 played a role in the survival on *P. aeruginosa* upon the knockdown of *eft-2* and *eef-1B.2*. While the knockdown of *eft-2* and *eef-1B.2* led to a reduction in the survival of N2 animals on *P. aeruginosa*, their knockdown did not alter the survival of *zip-2(tm4248)* animals (Figure 5C-5F). These results indicated that the diminished survival of *C. elegans* on *P. aeruginosa* upon the inhibition of translation elongation is mediated by ZIP-2.

Discussions

A large number of pathogens, including viruses and bacteria, block host translation (Mccormick & Khaperskyy 2017; Remick et al. 2023). The dampening of host translation may assist the pathogen in evading host immune responses, given that the synthesis of host immune effector polypeptides is concurrently suppressed. Since various pathogens target host protein synthesis, the blockade of translation might simulate a pathogen attack, consequently triggering the activation of immune responses. Indeed, the inhibition of protein synthesis, independent of pathogens, has been demonstrated to induce immune responses (Dunbar et al. 2012; Govindan et al. 2015; Melo & Ruvkun 2012). However, the mere elevation in the mRNA levels of immune genes may not serve as a reliable indicator of the host's ability to survive the pathogen attack. For example, the *Pseudomonas entomophila*-mediated blockade

of *Drosophila* protein synthesis resulted in an impaired immune response, notwithstanding the upregulation of mRNA levels of immune genes (Chakrabarti et al. 2012). Hence, it becomes imperative to couple the analysis of immune gene mRNA levels with the host's survival upon pathogen challenge following the inhibition of translation. In the current study, we demonstrate that, despite the increased mRNA levels of immune genes, inhibition of translation initiation and elongation can yield opposing outcomes in terms of host survival when challenged with a pathogen (Figure 6).

We have shown that inhibiting translation initiation enhances survival, while inhibiting translation elongation diminishes the survival of *C. elegans* on *P. aeruginosa*. Why would inhibition of translation initiation and elongation yield contrasting effects on *C. elegans* survival on *P. aeruginosa* when both interventions lead to increased mRNA levels of immune genes? One plausible explanation is that the inhibition of the elongation step produces toxic premature polypeptides (Svidritskiy et al. 2018), while inhibition of the initiation step decreases overall protein synthesis without generating premature peptides. However, since the adverse effects of inhibiting the elongation step are fully rescued by the knockdown of ZIP-2, it seems unlikely that reduced survival results from toxic byproducts. If toxic premature polypeptides were the primary cause, blocking ZIP-2-mediated immune responses would not be expected to reverse these adverse effects. Another possibility is that the survival on the pathogen hinges on the balance between increased energy consumption due to elevated mRNA synthesis for immune genes and the quantity of immune effector polypeptides produced upon inhibiting translation initiation and elongation. Nevertheless, since the inhibition of both initiation and elongation factors reduces *C. elegans* gut colonization with *P. aeruginosa*, it suggests that an effective immune response is likely generated when both steps are inhibited.

It is also conceivable that inhibiting translation elongation triggers the activation of a hyperimmune response mediated by ZIP-2, which proves detrimental to the host despite reducing gut colonization with *P. aeruginosa*. Indeed, inhibition of translation elongation has been shown to induce more robust immune responses than inhibition of initiation (Dunbar et al. 2012). The activation of hyperimmune responses has been demonstrated to reduce the survival of *C. elegans* on *P. aeruginosa* despite diminishing gut colonization by the bacterium (Rao et al. 2023). Given that the knockout of ZIP-2 reverses the adverse effects of inhibiting translation elongation on host survival, a hyperimmune response could underlie the detrimental effects of inhibiting translation elongation. However, our current study does not address how the same transcription factor, ZIP-2, results in opposing survival outcomes upon

inhibiting translation initiation and elongation. Future studies are required to elucidate the mechanisms underlying the reduced survival of *C. elegans* on *P. aeruginosa* upon inhibiting translation elongation.

Innate immunity appears to be a pivotal factor for enhanced lifespan (Garsin et al. 2003; Soo et al. 2023). Because the inhibition of translation contributes to an extended lifespan, it becomes crucial to discern whether the heightened lifespan resulting from translation blockage is attributable to an augmented immune response. Inhibition of both translation initiation and elongation is known to increase *C. elegans* lifespan (Li et al. 2011; Statzer et al. 2022). However, our findings reveal a dichotomy: while the inhibition of translation initiation enhances survival, the inhibition of translation elongation diminishes the survival of *C. elegans* on *P. aeruginosa*. Notably, the knockdown of *hel-1*, functioning as both an RNA helicase and a translation initiation factor, is known to reduce *C. elegans* lifespan by about 9% (Seo et al. 2015). On the other hand, our observations indicate that its knockdown extends *C. elegans* survival on *P. aeruginosa* by approximately 33% (Figure 1G). The translation initiation factor *ife-2*, known for increasing lifespan by about 18% (Matei et al. 2021), exhibits a distinct pattern. Although it extends lifespan, it does not alter the survival of *C. elegans* on *P. aeruginosa* (Figure 1G). These studies imply that pathways related to immunity may not necessarily mediate the increased lifespan resulting from translation inhibition. While ZIP-2 appears to be the major immune modulator when translation initiation and elongation are inhibited, several pathways work parallelly during translation inhibition to modulate lifespan (Hansen et al. 2007b; Rogers et al. 2011; Pan et al. 2007; Howard et al. 2016; Li et al. 2011). These observations suggest that translation inhibition-mediated longevity and pathogen resistance are regulated by distinct genetic mechanisms.

Materials and methods

Bacterial strains

The bacterial strains utilized in this study include *Escherichia coli* OP50, *E. coli* HT115(DE3), *Pseudomonas aeruginosa* PA14, *P. aeruginosa* PA14 expressing green fluorescent protein (*P. aeruginosa* PA14-GFP). The cultures of *E. coli* OP50, *E. coli* HT115(DE3), and *P. aeruginosa* PA14 were grown in Luria-Bertani (LB) broth at 37°C, while the cultures of *P. aeruginosa* PA14-GFP were grown in LB broth with 50 µg/mL kanamycin at 37°C.

C. elegans strains and growth conditions

C. elegans hermaphrodites were maintained at 20°C on nematode growth medium (NGM) plates seeded with *E. coli* OP50 as the food source unless otherwise indicated. The wild-type control used was Bristol N2. The following strains were used in the study: *zip-2(tm4248),* KU25 *pmk-1(km25),* NU3 *dbl-1(nk3),* AE501 *nhr-8(ok186),* KU4 *sek-1(km4),* and HC196 *sid-1(qt9).* All the strains were obtained from the Caenorhabditis Genetics Center (University of Minnesota, Minneapolis, MN) except for *zip-2(tm4248*), which was obtained from the National BioResearch Project (*C. elegans*), Japan.

C. elegans development assays

Wild-type N2 gravid hermaphrodites were lysed in an alkaline bleach solution to obtain eggs, which were then washed three times with the M9 buffer solution. The eggs were then incubated in the M9 buffer solution for 22 hours at room temperature in a 1.5 mL microcentrifuge tube to obtain synchronized L1-arrested worms. These synchronized L1 worms were then transferred to RNAi plates targeting different translation factors and incubated at 20°C for 72 hours. Following this, animals were scored for normal or slowed development. At least three independent experiments (biological replicates) were performed for each condition.

RNA interference (RNAi)

RNAi was employed to induce loss-of-function phenotypes by feeding worms with the *E. coli* strain HT115(DE3) expressing double-stranded RNA homologous to a target *C. elegans* gene. The list of *C. elegans* genes encoding translation factors was obtained from (Rhoads et al. 2006). RNAi was carried out as described previously (Das et al. 2023). Briefly, *E. coli* HT115(DE3) with the appropriate vectors were grown in LB broth containing ampicillin (100 μg/mL) at 37°C overnight on a shaker, concentrated ten times, and plated onto RNAi NGM plates containing 100 μg/mL ampicillin and 3 mM isopropyl β-D-thiogalactoside (IPTG). The plated bacteria were allowed to grow overnight at 37°C. Out of 47 translation factors, the knockdown of 23 led to the slowed development of worms. Therefore, for the genes whose knockdown led to slowed development (Table S1), the worms were grown on the empty vector control RNAi until the L3 stage before being transferred to the corresponding gene RNAi. The worms were grown on RNAi bacteria till the 1-day-adult stage before being utilized for subsequent experiments. The eggs were allowed to develop at 20°C for 96 hours on RNAi for the genes whose knockdown did not affect development, except for *eef-1B.2*.

For comparison with *eft-2*, RNAi against *eef-1B*.2 was initiated from the L3 stage. The RNAi clones were from the Ahringer RNAi library and were verified by sequencing.

C. elegans killing assays on _P. aeruginosa_ PA14

The full-lawn killing assays of *C. elegans* on *P. aeruginosa* PA14 were conducted as described earlier (Singh & Aballay 2019a). Briefly, bacterial cultures were prepared by inoculating individual bacterial colonies of *P. aeruginosa* into 3 mL of LB and grown for 10-12 hours on a shaker at 37°C. Bacterial lawns were prepared by spreading 20 µL of the culture on the entire surface of 3.5-cm-diameter modified NGM agar plates (0.35% instead of 0.25% peptone). The plates were incubated at 37°C for 10-12 hours and then cooled to room temperature for at least 30 minutes before seeding with synchronized 1-day-old adult animals. The killing assays were carried out at 25°C, and live animals were transferred daily to fresh *P. aeruginosa* plates. Animals were scored at times indicated and were considered dead when they failed to respond to touch. At least three independent experiments (biological replicates) were performed for each condition.

P. aeruginosa-GFP colonization assay

The *P. aeruginosa* PA14-GFP colonization assays were carried out as described earlier (Rao et al. 2023; Singh & Aballay 2019b). Briefly, bacterial cultures were prepared by inoculating individual bacterial colonies of *P. aeruginosa* PA14-GFP into 3 mL of LB containing 50 µg/mL kanamycin and grown for 10-12 hours on a shaker at 37°C. Bacterial lawns were prepared by spreading 20 µL of the culture on the entire surface of 3.5-cm-diameter modified NGM agar plates (0.35% instead of 0.25% peptone) containing 50 µg/mL of kanamycin. The plates were incubated at 37°C for 12 hours and then cooled to room temperature for at least 30 minutes before seeding with 1-day-old adult gravid adults. The assays were performed at 25°C. At indicated times, the worms were picked under a non-fluorescence stereomicroscope and visualized within 5 minutes under a fluorescence microscope. At least three independent experiments (biological replicates) were performed for each condition.

RNAi efficiency test for _zip-2(tm4248)_

The wild-type N2 and *zip-2(tm4248)* animals were synchronized by egg laying on *act-5* and *bli-3* RNAi plates along with the empty vector control RNAi plates. The *sid-1(qt9)* animals were used as RNAi-defective controls (Whangbo et al. 2017). The plates with eggs were

incubated at 20°C for 72 hours. After that, the animals were monitored for development defects and blisters on the cuticle for *act-5* and *bli-3* RNAi, respectively.

C. elegans RNA isolation and quantitative reverse transcription-PCR (qRT-PCR)

Both wild-type N2 and *zip-2(tm4248)* animals were synchronized by egg-laying. Approximately 50 gravid adult animals were transferred to 9-cm control empty vector RNAi plates and allowed to lay eggs for 4 hours. The gravid adults were then removed, and the eggs were allowed to develop at 20°C for 36 hours (until the L3 stage). After that, the synchronized L3 animals were collected in M9, washed twice with M9, and transferred to 9-cm *eif-2α, ifg-1, eft-2,* and *eef-1B.2* RNAi plates and were allowed to grow till 1-day-old adults. The control animals were maintained on the empty vector RNAi till they grew to 1-day-old adults. Subsequently, the animals were collected, washed with M9 buffer, and frozen in TRIzol reagent (Life Technologies, Carlsbad, CA). Total RNA was extracted using the RNeasy Plus Universal Kit (Qiagen, Netherlands). A total of 1 μg of total RNA was reverse-transcribed with random primers using the PrimeScript™ 1st strand cDNA Synthesis Kit (TaKaRa) according to the manufacturer's protocols. qRT-PCR was conducted using TB Green fluorescence (TaKaRa) on a MasterCycler EP Realplex 4 thermal cycler (Eppendorf) in 96-well-plate format. Fifteen microliter reactions were analyzed as outlined by the manufacturer (TaKaRa). The relative fold-changes of the transcripts were calculated using the comparative $CT(2^{-\Delta\Delta}CT)$ method and normalized to pan-actin (*act-1, -3, -4*) as described earlier (Singh & Aballay 2017). All samples were run in triplicate (technical replicates) and repeated at least four times (biological replicates). The sequence of the primers is provided in Table S3.

Fluorescence imaging of _C. elegans_

Fluorescence imaging was carried out as described previously (Gokul & Singh 2022; Ravi et al. 2023). Briefly, the animals were picked under a non-fluorescence stereomicroscope to avoid potential bias. The animals were anesthetized using an M9 salt solution containing 50 mM sodium azide and mounted onto 2% agarose pads. The animals were then visualized using a Nikon SMZ-1000 fluorescence stereomicroscope. The fluorescence intensity was quantified using Image J software.

Quantification and statistical analysis

The statistical analysis was performed with Prism 8 (GraphPad). All error bars represent the mean ± standard deviation (SD). The two-sample *t*-test was employed when needed, and statistical significance was determined when $P < 0.05$. In the figures, asterisks (*) denote statistical significance as follows: *, $P < 0.05$, **, $P < 0.01$, ***, $P < 0.001$, as compared with the appropriate controls. The Kaplan-Meier method was utilized to calculate the survival fractions, and statistical significance between survival curves was determined using the log-rank test. All experiments were performed at least three times unless otherwise indicated.

Author contributions

A.G. and J.S. conceived and designed the experiments. A.G. performed the experiments. A.G. and J.S. analyzed the data and wrote the paper.

Acknowledgments

We thank the Caenorhabditis Genetics Center (funded by the NIH Office of Research Infrastructure Programs (P40 OD010440)) and the National BioResearch Project (*C. elegans*), Japan, for providing the strains used in this study.

Funding

This work was supported by the following grants: Ramalingaswami Re-entry Fellowship (Ref. No. BT/RLF/Re-entry/50/2020) awarded by the Department of Biotechnology, India; STARS grant (File No. MoE-STARS/STARS-2/2023-0116) awarded by the Ministry of Education, India; Research Grant (Ref. No. 37/1741/23/EMR-II) awarded by the Council of Scientific & Industrial Research (CSIR), India; and IISER Mohali intramural funds. A.G. was supported by a senior research fellowship from the CSIR, India.

Conflict of interest statement

The authors declare no competing interests.

Data availability statement

All data generated or analyzed during this study are included in the manuscript and supporting files.

References

Blazie SM, Takayanagi-Kiya S, McCulloch KA & Jin Y (2021) Eukaryotic initiation factor EIF-3.G augments mRNA translation efficiency to regulate neuronal activity. *Elife* 10, e68336.

Buttgereit F & Brandt MD (1995) A hierarchy of ATP-consuming. *Biochem. J.* 312, 163–167.

Cattie DJ, Richardson CE, Reddy KC, Ness-Cohn EM, Droste R, Thompson MK, Gilbert W V. & Kim DH (2016) Mutations in Nonessential eIF3k and eIF3l Genes Confer Lifespan Extension and Enhanced Resistance to ER Stress in Caenorhabditis elegans. *PLoS Genet.* 12, e1006326.

Chakrabarti S, Liehl P, Buchon N & Lemaitre B (2012) Infection-induced host translational blockage inhibits immune responses and epithelial renewal in the Drosophila gut. *Cell Host Microbe* 12, 60–70. Available at: http://dx.doi.org/10.1016/j.chom.2012.06.001.

Clay KJ, Yang Y, Clark C & Petrascheck M (2023) Proteostasis is differentially modulated by inhibition of translation initiation or elongation. *Elife* 12, e76465.

Contreras V, Richardson MA, Hao E & Keiper BD (2008) Depletion of the cap-associated isoform of translation factor eIF4G induces germline apoptosis in C. elegans. *Cell Death Differ.* 15, 1232–1242.

Curran SP & Ruvkun G (2007) Lifespan regulation by evolutionarily conserved genes essential for viability. *PLoS Genet.* 3, e56.

Das P, Aballay A & Singh J (2023) Calcineurin inhibition enhances Caenorhabditis elegans lifespan by defecation defects-mediated calorie restriction and nuclear hormone signaling. *Elife* 12, RP89572.

Dunbar TL, Yan Z, Balla KM, Smelkinson MG & Troemel ER (2012) C. elegans detects pathogen-induced translational inhibition to activate immune signaling. *Cell Host Microbe* 11, 375–386.

Estes KA, Dunbar TL, Powell JR, Ausubel FM & Troemel ER (2010) bZIP transcription factor zip-2 mediates an early response to Pseudomonas aeruginosa infection in Caenorhabditis elegans. *Proc. Natl. Acad. Sci. USA* 107, 2153–2158.

Fontana MF, Banga S, Barry KC, Shen X, Tan Y, Luo Z & Vance RE (2011) Secreted Bacterial Effectors That Inhibit Host Protein Synthesis Are Critical for Induction of the Innate Immune Response to Virulent Legionella pneumophila. *PLoS Pathog.* 7, e1001289.

Garsin DA, Villanueva JM, Begun J, Kim DH, Sifri CD, Calderwood SB, Ruvkun G & Ausubel FM (2003) Long-Lived C. elegans daf-2 Mutants Are Resistant to Bacterial

Pathogens. *Science (80-.).* 300, 1921.

Gebauer F & Hentze MW (2004) MOLECULAR MECHANISMS OF TRANSLATIONAL CONTROL. *Nat. Rev. Mol. Cell Biol.* 5, 827–835.

Gokul G & Singh J (2022) Dithiothreitol causes toxicity in C. elegans by modulating the methionine-homocysteine cycle. *Elife* 11, e76021.

Gonskikh Y & Polacek N (2017) Alterations of the translation apparatus during aging and stress response. *Mech. Ageing Dev.* 168, 30–36. Available at: https://doi.org/10.1016/j.mad.2017.04.003.

Govindan JA, Jayamani E, Zhang X, Breen P, Larkins-Ford J, Mylonakis E & Ruvkun G (2015) Lipid signalling couples translational surveillance to systemic detoxification in Caenorhabditis elegans. *Nat. Cell Biol.* 17, 1294–1303.

Hansen M, Taubert S, Crawford D, Libina N, Lee SJ & Kenyon C (2007a) Lifespan extension by conditions that inhibit translation in Caenorhabditis elegans. *Aging Cell* 6, 95–110.

Hansen M, Taubert S, Crawford D, Libina N, Lee SJ & Kenyon C (2007b) Lifespan extension by conditions that inhibit translation in Caenorhabditis elegans. *Aging Cell* 6, 95–110.

Howard AC, Rollins J, Snow S, Castor S & Rogers AN (2016) Reducing translation through eIF4G/IFG-1 improves survival under ER stress that depends on heat shock factor HSF-1 in Caenorhabditis elegans. *Aging Cell* 15, 1027–1038.

Jackson RJ, Hellen CUT & Pestova T V. (2010) The mechanism of eukaryotic translation initiation and principles of its regulation. *Nat. Rev. Mol. Cell Biol.* 10, 113–127.

Johnstone O & Lasko P (2004) Interaction with eIF5B is essential for Vasa function during development. *Development* 131, 4167–4178.

Kim DH, Feinbaum R, Emerson FE, Garsin DA, Inoue H, Tanaka-hino M, Hisamoto N, Matsumoto K, Tan M-W & Ausubel FM (2002) A Conserved p38 MAP Kinase Pathway in Caenorhabditis elegans Innate Immunity. *Science (80-.).* 297, 623–627.

Knight JRP, Garland G, Po T, Mead E, Vlahov N, Sfakianos A, Grosso S, De-lima-hedayioglu F, Mallucci GR, Haar T Von Der, Smales CM, Sansom OJ & Willis AE (2020) Control of translation elongation in health and disease. *Dis. Model. Mech.* 13, dmm043208.

Li X, Matilainen O, Jin C, Glover-Cutter KM, Holmberg CI & Blackwell TK (2011) Specific SKN-1/Nrf stress responses to perturbations in translation elongation and proteasome activity. *PLoS Genet.* 7, e1002119.

Liu Z, Dong Z, Yang Z, Chen Q, Pan Y, Yang Y, Cui P, Zhang X & Zhang J-T (2007) Role of eIF3a (eIF3 p170) in intestinal cell differentiation and its association with early development. *Differentiation* 75, 652–661. Available at: http://dx.doi.org/10.1111/j.1432-0436.2007.00165.x.

Long X, Spycher C, Han ZS, Rose AM, Mu F & Avruch J (2002) TOR Deficiency in C. elegans Causes Developmental Arrest and Intestinal Atrophy by Inhibition of mRNA Translation. *Curr. Biol.* 12, 1448–1461.

Mallo G V, Kurz CL, Couillault C, Pujol N, Granjeaud S, Kohara Y & Ewbank JJ (2002) Inducible Antibacterial Defense System in C. elegans. *Curr. Biol.* 12, 1209–1214.

Martinez-Miguel VE, Lujan C, Espie–Caullet T, Martinez-Martinez D, Moore S, Backes C, Gonzalez S, Galimov ER, Brown AEX, Halic M, Tomita K, Rallis C, von der Haar T, Cabreiro F & Bjedov I (2021) Increased fidelity of protein synthesis extends lifespan. *Cell Metab.* 33, 2288-2300.e12.

Matei IV, Netsai V, Samukange C, Bunu G, Toren D, Ghenea S & Tacutu R (2021) Knock-down of odr-3 and ife-2 additively extends lifespan and healthspan in C. elegans. *Aging (Albany. NY).* 13, 21040–21065.

Mccormick C & Khaperskyy DA (2017) Translation inhibition and stress granules in the antiviral immune response. *Nat. Rev. Immunol.* 17, 647–660.

McEwan DL, Kirienko N V & Ausubel FM (2012) Host Translational Inhibition by Pseudomonas aeruginosa Exotoxin A Triggers an Immune Response in Caenorhabditis elegans. *Cell Host Microbe* 11, 364–374. Available at: http://dx.doi.org/10.1016/j.chom.2012.02.007.

Melo JA & Ruvkun G (2012) Inactivation of Conserved C . elegans Genes Engages Pathogen- and Xenobiotic-Associated Defenses. *Cell* 149, 452–466. Available at: http://dx.doi.org/10.1016/j.cell.2012.02.050.

Miyata S, Begun J, Troemel ER & Ausubel FM (2008) DAF-16-dependent suppression of immunity during reproduction in Caenorhabditis elegans. *Genetics* 178, 903–918.

Mohr I & Sonenberg N (2012) Host Translation at the Nexus of Infection and Immunity. *Cell Host Microbe* 12, 470–483. Available at: http://dx.doi.org/10.1016/j.chom.2012.09.006.

Otarigho B & Aballay A (2020) Cholesterol Regulates Innate Immunity via Nuclear Hormone Receptor NHR-8. *iScience* 23, 101068. Available at: https://doi.org/10.1016/j.isci.2020.101068.

Pakos-Zebrucka K, Koryga I, Mnich K, Ljujic M, Samali A & Gorman AM (2016) The integrated stress response. *EMBO Rep.* 17, 1374–1395.

Pan KZ, Palter JE, Rogers AN, Olsen A, Chen D, Lithgow GJ & Kapahi P (2007) Inhibition of mRNA translation extends lifespan in Caenorhabditis elegans. *Aging Cell* 6, 111–119.

Peterson ND, Icso JD, Salisbury JE, Rodríguez T, Thompson PR & Pukkila-Worley R (2022) Pathogen infection and cholesterol deficiency activate the C. elegans p38 immune pathway through a TIR-1/SARM1 phase transition. *Elife* 11, e74206.

Rao R, Aballay A & Singh J (2023) Inhibition of the UFD-1-NPL-4 complex triggers an inflammation-like response in Caenorhabditis elegans. *bioRxiv* 12.12.5712, doi.org/10.1101/2023.12.12.571255.

Ravi, Kumar A, Bhattacharyya S & Singh J (2023) Thiol reductive stress activates the hypoxia response pathway. *EMBO J.* 42, e114093.

Remick BC, Gaidt MM & Vance RE (2023) Effector-Triggered Immunity. *Annu. Rev. Immunol.* 41, 453–481.

Rhoads RE, Dinkova TD & Korneeva NL (2006) Mechanism and regulation of translation in C. elegans. In *WormBook*. pp.1–18.

Rogers AN, Chen D, McColl G, Czerwieniec G, Felkey K, Gibson BW, Hubbard A, Melov S, Lithgow GJ & Kapahi P (2011) Life span extension via eIF4G inhibition is mediated by posttranscriptional remodeling of stress response gene expression in C. elegans. *Cell Metab.* 14, 55–66.

Seo M, Seo K, Hwang W, Koo HJ, Hahm J, Yang J, Han SK, Hwang D, Kim S, Jang SK, Lee Y, Nam HG & Lee S-J V. (2015) RNA helicase HEL-1 promotes longevity by specifically activating DAF-16/FOXO transcription factor signaling in Caenorhabditis elegans. *Proc. Natl. Acad. Sci. USA* 112, E4246–E4255.

Simmer F, Moorman C, Van Der Linden AM, Kuijk E, Van Den Berghe PVE, Kamath RS, Fraser AG, Ahringer J & Plasterk RHA (2003) Genome-wide RNAi of C. elegans using the hypersensitive rrf-3 strain reveals novel gene functions. *PLoS Biol.* 1, 77–84.

Singh J (2020) Phase Separation of RNA Helicase Triggers Stress-Responsive Translational Switch. *Trends Biochem. Sci.* 45, 726–728. Available at: https://doi.org/10.1016/j.tibs.2020.06.008.

Singh J & Aballay A (2017) Endoplasmic reticulum stress caused by lipoprotein accumulation suppresses immunity against bacterial pathogens and contributes to immunosenescence. *MBio* 8, e00778-17.

Singh J & Aballay A (2019a) Intestinal infection regulates behavior and learning via neuroendocrine signaling. *Elife* 8, e50033.

Singh J & Aballay A (2019b) Microbial colonization activates an immune fight-and-flight

response via neuroendocrine signaling. *Dev. Cell* 49, 89–99.

Soo SK, Traa A, Rudich ZD, Moldakozhayev A, Mistry M & Raamsdonk JM Van (2023) Genetic basis of enhanced stress resistance in long-lived mutants highlights key role of innate immunity in determining longevity. *Aging Cell* 22, e13740.

Spriggs KA, Bushell M & Willis AE (2010) Translational Regulation of Gene Expression during Conditions of Cell Stress. *Mol. Cell* 40, 228–237. Available at: http://dx.doi.org/10.1016/j.molcel.2010.09.028.

Starck SR, Tsai JC, Chen K, Shodiya M, Wang L, Yahiro K, Martins-Green M, Shastri N & Walter P (2016) Translation from the 5' untranslated region shapes the integrated stress response. *Science (80-.).* 351, aad3867-1-aad3867-10.

Statzer C, Meng J, Venz R, Bland M, Robida-stubbs S, Patel K, Petrovic D, Emsley R, Liu P, Morantte I, Haynes C, Mair WB, Longchamp A, Filipovic MR, Blackwell TK & Ewald CY (2022) ATF-4 and hydrogen sulfide signalling mediate longevity in response to inhibition of translation or mTORC1. *Nat. Commun.* 13, 967.

Svidritskiy E, Demo G & Korostelev AA (2018) Mechanism of premature translation termination on a sense codon. *J. Biol. Chem.* 293, 12472–12479. Available at: http://dx.doi.org/10.1074/jbc.AW118.003232.

Tan M-W, Mahajan-Miklos S & Ausubel FM (1999) Killing of Caenorhabditis elegans by Pseudomonas aeruginosa used to model mammalian bacterial pathogenesis. *Proc. Natl. Acad. Sci. USA* 96, 715–720.

Whangbo JS, Weisman AS, Chae J & Hunter CP (2017) SID-1 domains important for dsRNA import in Caenorhabditis elegans. *G3 Genes, Genomes, Genet.* 7, 3887–3899.

Xie J, de Souza Alves V, von der Haar T, O'Keefe L, Lenchine R V., Jensen KB, Liu R, Coldwell MJ, Wang X & Proud CG (2019) Regulation of the Elongation Phase of Protein Synthesis Enhances Translation Accuracy and Modulates Lifespan. *Curr. Biol.* 29, 737-749.e5.

Figures

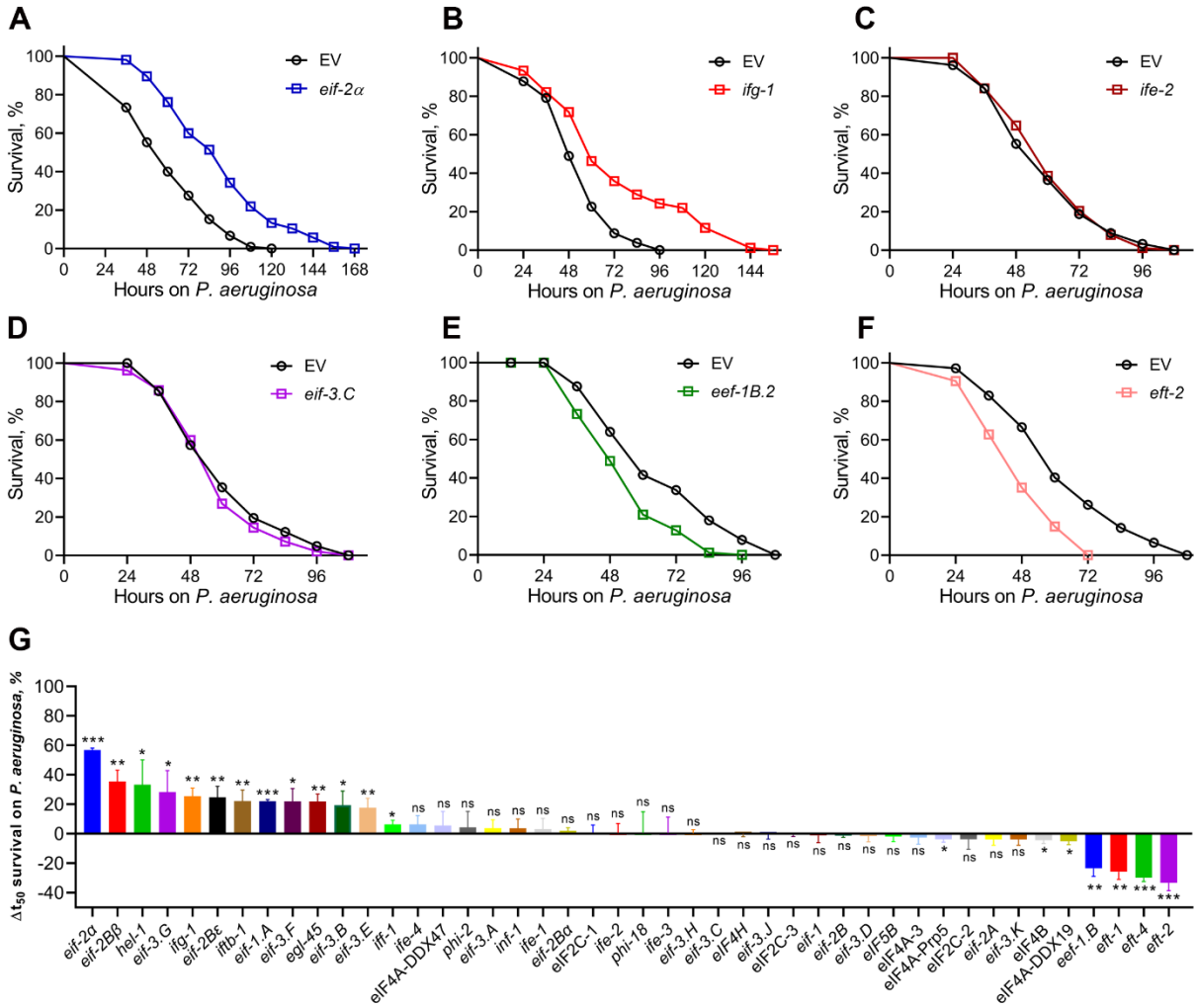

Figure 1. Inhibition of translation initiation or elongation leads to opposing outcomes on *C. elegans* survival during *P. aeruginosa* infection

(A)-(F) Representative survival plots of N2 animals on *P. aeruginosa* PA14 at 25°C after treatment with *eif-2α* (A), *ifg-1* (B), *ife*-2 (C), *eif-3.C* (D), *eef-1B.2* (E), and *eft-2* (F) RNAi, along with the empty vector (EV) control. *P* values for different gene knockdowns compared to the corresponding EV control are as follows: $P<0.001$ for *eif-2α*, *ifg-1*, *eef-1B.2*, and *eft-2*. Survival curves for *ife-2* and *eif-3.C* RNAi compared to EV control are nonsignificant. (G) The percent mean survival change on *P. aeruginosa* upon the knockdown of different initiation and elongation factors compared to the EV control. ***$P < 0.001$, **$P < 0.01$, and *$P < 0.05$ via the *t*-test. ns, nonsignificant. Data represent the mean and standard deviation from three independent experiments. The triplicate data is available in Table S2.

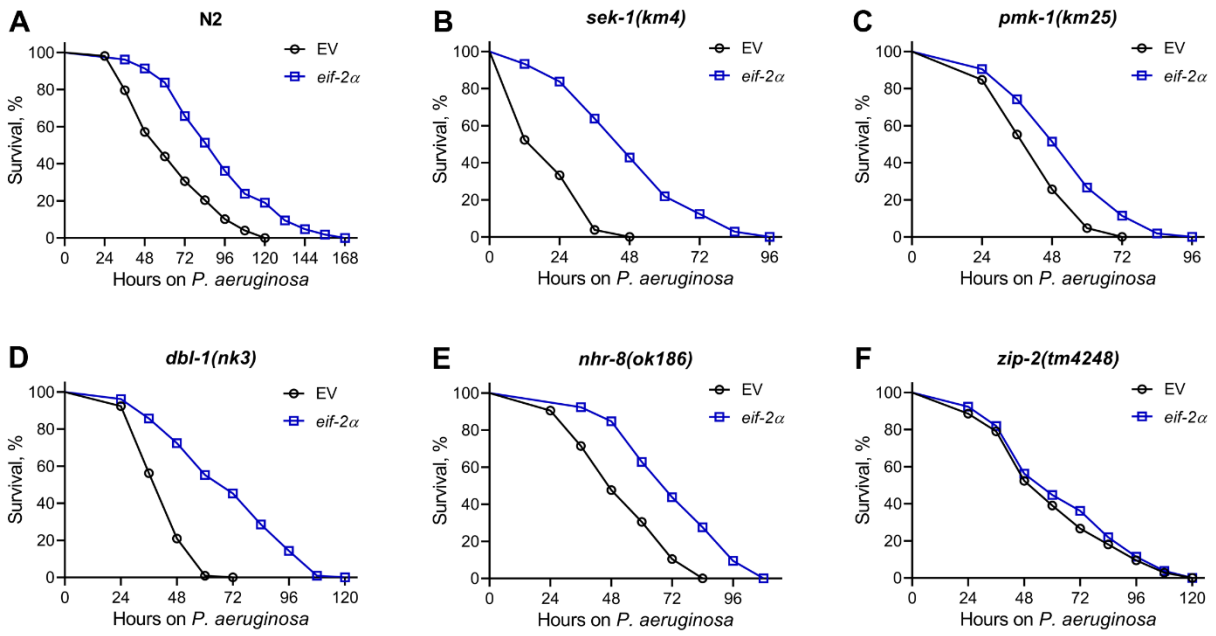

Figure 2. Knockdown of *eif-2α* increases *C. elegans* survival on *P. aeruginosa* via transcription factor ZIP-2

Representative survival plots of N2 (A), *sek-1(km4)* (B), *pmk-1(km25)* (C), *dbl-1(nk3)* (D), *nhr-8(ok186)* (E), and *zip-2(tm4248)* (F) animals on *P. aeruginosa* PA14 at 25°C after treatment with the empty vector (EV) control and *eif-2α* RNAi. $P<0.001$ for *eif-2α* RNAi compared to EV control for N2, *sek-1(km4)*, *pmk-1(km25)*, *dbl-1(nk3)*, and *nhr-8(ok186)*. Survival curves for *eif-2α* RNAi compared to EV control for *zip-2(tm4248)* are nonsignificant.

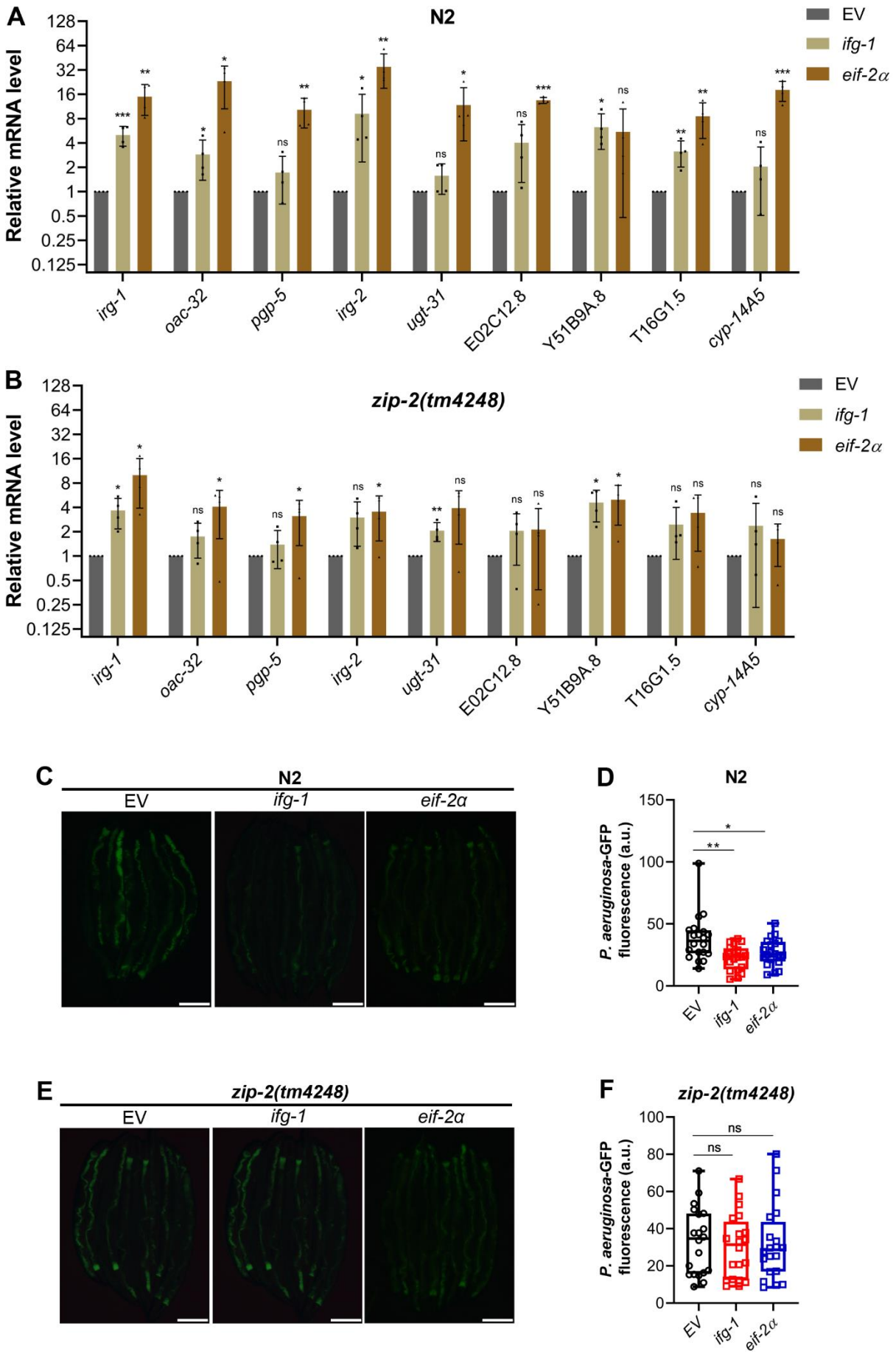
A
N2
Relative mRNA level
128
64
32
16
8
4
2
1
0.5
0.25
0.125
EV
ifg-1
eif-2α
irg-1
oac-32
pgp-5
irg-2
ugt-31
E02C12.8
Y51B9A.8
T16G1.5
cyp-14A5
B
zip-2(tm4248)
C
N2
EV
ifg-1
eif-2α
D
N2
P. aeruginosa-GFP fluorescence (a.u.)
150
100
50
0
E
zip-2(tm4248)
F
zip-2(tm4248)
ns

624

Figure 3. Inhibition of translation initiation reduces *C. elegans* gut colonization with *P. aeruginosa* by activating immune response genes via ZIP-2

(A)-(B) Immune gene expression analysis of N2 (A) and *zip-2(tm4248)* (B) animals after treatment with the empty vector (EV) control, *ifg-1*, and *eif-2α* RNAi. ***$P < 0.001$, **$P < 0.01$, and *$P < 0.05$ via the *t*-test. ns, nonsignificant. Data represent the mean and standard deviation from four independent experiments.

(C) Representative fluorescence images of N2 animals incubated on *P. aeruginosa*-GFP for 24 hours at 25°C after treatment with the EV control, *ifg-1*, and *eif-2α* RNAi. Scale bar = 200 μm.

(D) Quantification of GFP levels of N2 animals incubated on *P. aeruginosa*-GFP for 24 hours at 25°C after treatment with the EV control, *ifg-1*, and *eif-2α* RNAi. **$P < 0.01$ and *$P < 0.05$ via the *t*-test ($n = 20$ worms each).

(E) Representative fluorescence images of *zip-2(tm4248)* animals incubated on *P. aeruginosa*-GFP for 24 hours at 25°C after treatment with the EV control, *ifg-1*, and *eif-2α* RNAi. Scale bar = 200 μm.

(F) Quantification of GFP levels of *zip-2(tm4248)* animals incubated on *P. aeruginosa*-GFP for 24 hours at 25°C after treatment with the EV control, *ifg-1*, and *eif-2α* RNAi. ns, nonsignificant via the *t*-test ($n = 20$ worms each).

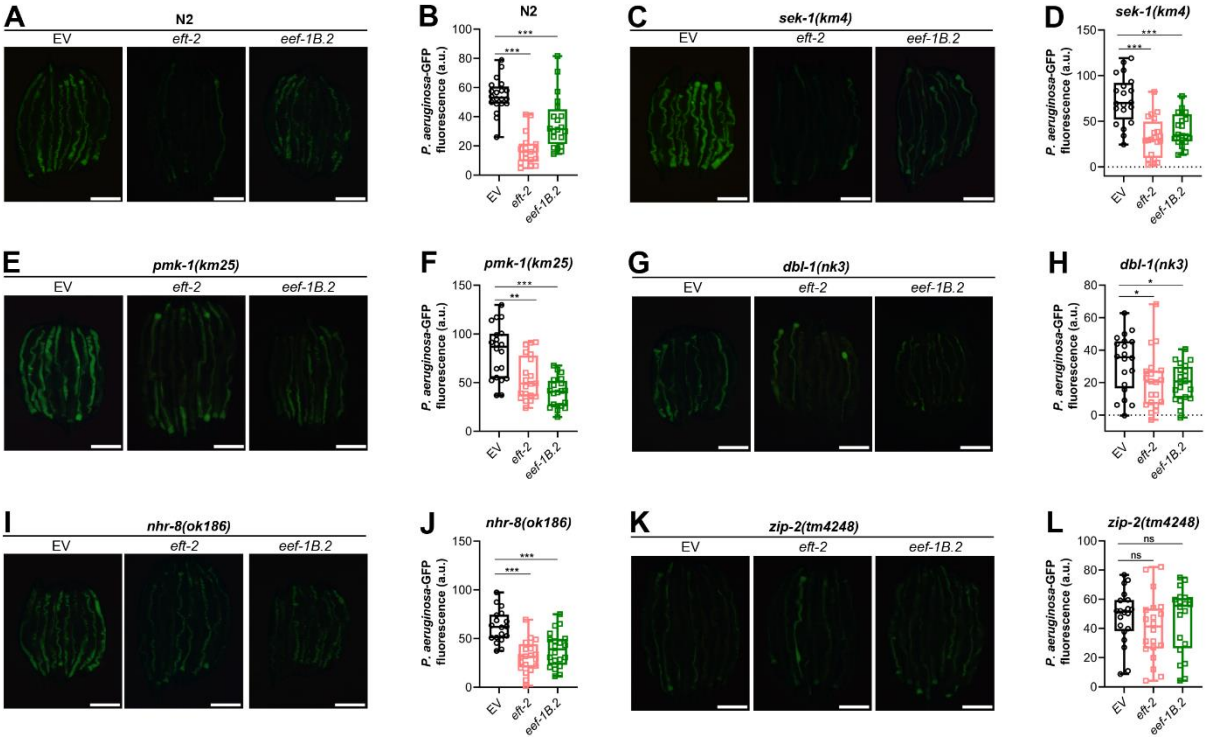

Figure 4. ZIP-2 reduces gut colonization with *P. aeruginosa* upon inhibition of translation elongation

(A) Representative fluorescence images of N2 animals incubated on *P. aeruginosa*-GFP for 24 hours at 25°C after treatment with the empty vector (EV) control, *eft-2*, and *eef-1B.2* RNAi. Scale bar = 200 μm.

(B) Quantification of GFP levels of N2 animals incubated on *P. aeruginosa*-GFP for 24 hours at 25°C after treatment with the EV control, *eft-2*, and *eef-1B.2* RNAi. ***$P < 0.001$ via the *t*-test ($n = 20$ worms each for EV and *eef-1B.2*, and 17 worms for *eft-2*).

(C) Representative fluorescence images of *sek-1(km4)* animals incubated on *P. aeruginosa*-GFP for 12 hours at 25°C after treatment with the EV control, *eft-2*, and *eef-1B.2* RNAi. Scale bar = 200 μm.

(D) Quantification of GFP levels of *sek-1(km4)* animals incubated on *P. aeruginosa*-GFP for 12 hours at 25°C after treatment with the EV control, *eft-2*, and *eef-1B.2* RNAi. ***$P < 0.001$ and via the *t*-test ($n = 20$ worms each).

(E) Representative fluorescence images of *pmk-1(km25)* animals incubated on *P. aeruginosa*-GFP for 24 hours at 25°C after treatment with the EV control, *eft-2*, and *eef-1B.2* RNAi. Scale bar = 200 μm.

(F) Quantification of GFP levels of *pmk-1(km25)* animals incubated on *P. aeruginosa*-GFP for 24 hours at 25°C after treatment with the EV control, *eft-2*, and *eef-1B.2* RNAi. ***$P < 0.001$ and **$P < 0.01$ via the *t*-test ($n = 20$ worms each).

(G) Representative fluorescence images of *dbl-1(nk3)* animals incubated on *P. aeruginosa*-GFP for 24 hours at 25°C after treatment with the EV control, *eft-2*, and *eef-1B.2* RNAi. Scale bar = 200 μm.

(H) Quantification of GFP levels of *dbl-1(nk3)* animals incubated on *P. aeruginosa*-GFP for 24 hours at 25°C after treatment with the EV control, *eft-2*, and *eef-1B.2* RNAi. $*P < 0.05$ via the *t*-test ($n = 20$ worms each).

(I) Representative fluorescence images of *nhr-8(ok186)* animals incubated on *P. aeruginosa*-GFP for 24 hours at 25°C after treatment with the EV control, *eft-2*, and *eef-1B.2* RNAi. Scale bar = 200 μm.

(J) Quantification of GFP levels of *nhr-8(ok186)* animals incubated on *P. aeruginosa*-GFP for 24 hours at 25°C after treatment with the EV control, *eft-2*, and *eef-1B.2* RNAi. $***P < 0.001$ via the *t*-test ($n = 20$ worms each for *eft-2* and *eef-1B.2*, and 18 worms for EV).

(K) Representative fluorescence images of *zip-2(tm4248)* animals incubated on *P. aeruginosa*-GFP for 24 hours at 25°C after treatment with the EV control, *eft-2*, and *eef-1B.2* RNAi. Scale bar = 200 μm.

(L) Quantification of GFP levels of *zip-2(tm4248)* animals incubated on *P. aeruginosa*-GFP for 24 hours at 25°C after treatment with the EV control, *eft-2*, and *eef-1B.2* RNAi. ns, nonsignificant via the *t*-test ($n = 20$ worms each).

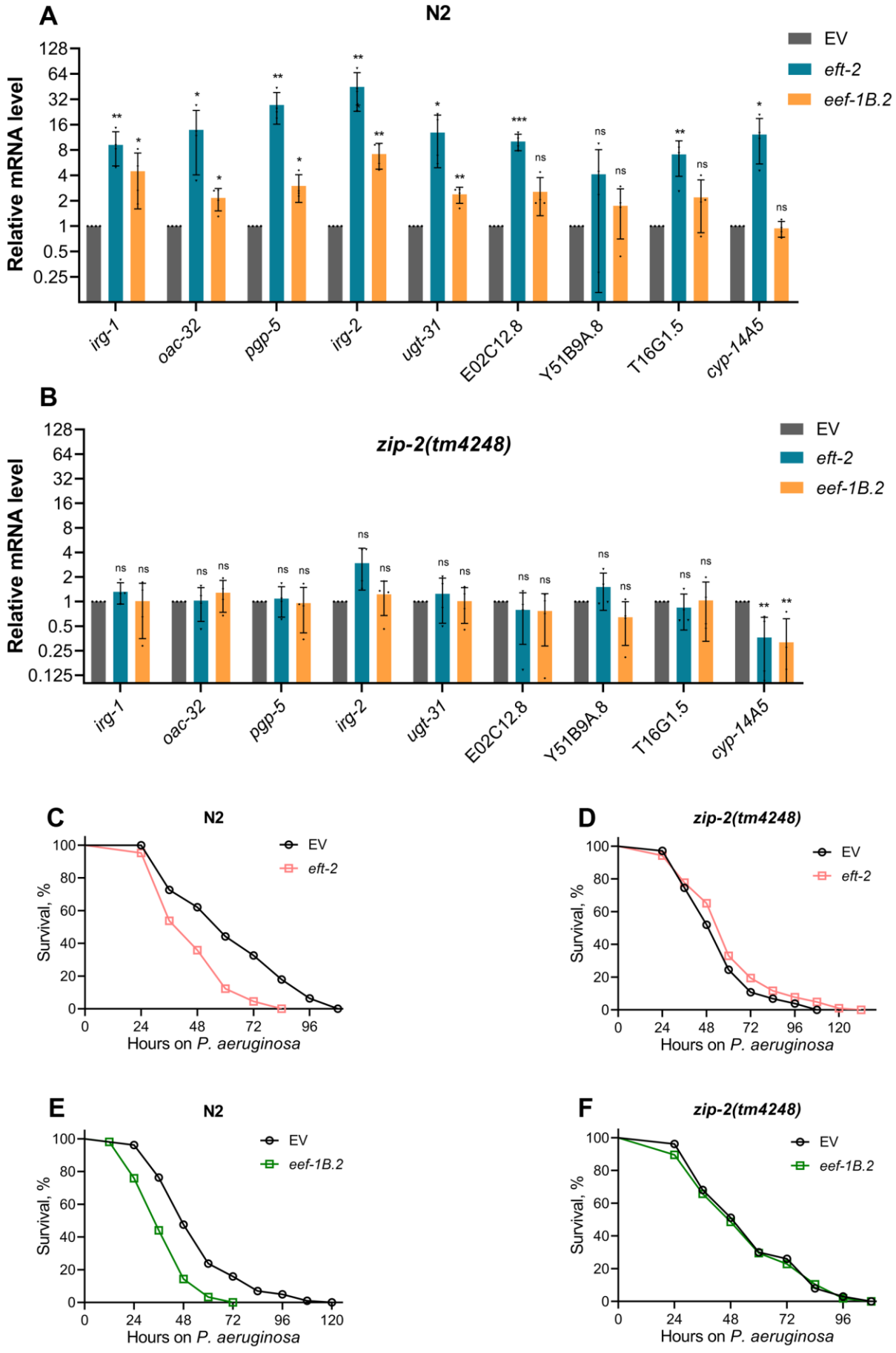
A
N2
EV
eft-2
eef-1B.2
Relative mRNA level
irg-1
oac-32
pgp-5
irg-2
ugt-31
E02C12.8
Y51B9A.8
T16G1.5
cyp-14A5
B
zip-2(tm4248)
C
D
E
F
Survival, %
Hours on P. aeruginosa
eef-1B.2

682

Figure 5. Inhibition of translation elongation reduces *C. elegans* survival on *P. aeruginosa* via ZIP-2

(A)-(B) Immune gene expression analysis of N2 (A) and *zip-2(tm4248)* (B) animals after treatment with the empty vector (EV) control, *eft-2*, and *eef-1B.2* RNAi. ***$P < 0.001$, **$P < 0.01$, and *$P < 0.05$ via the *t*-test. ns, nonsignificant. Data represent the mean and standard deviation from four independent experiments.

(C) Representative survival plots of N2 animals on *P. aeruginosa* PA14 at 25°C after treatment with the EV control and *eft-2* RNAi. $P<0.001$ for *eft-2* RNAi compared to EV control.

(D) Representative survival plots of *zip-2(tm4248)* animals on *P. aeruginosa* PA14 at 25°C after treatment with the EV control and *eft-2* RNAi. $P<0.05$ for *eft-2* RNAi compared to EV control.

(E) Representative survival plots of N2 animals on *P. aeruginosa* PA14 at 25°C after treatment with the EV control and *eef-1B.2* RNAi. $P<0.001$ for *eef-1B.2* RNAi compared to EV control.

(F) Representative survival plots of *zip-2(tm4248)* animals on *P. aeruginosa* PA14 at 25°C after treatment with the EV control and *eef-1B.2* RNAi. Survival curves for *eef-1B.2* RNAi compared to the EV control are nonsignificant.

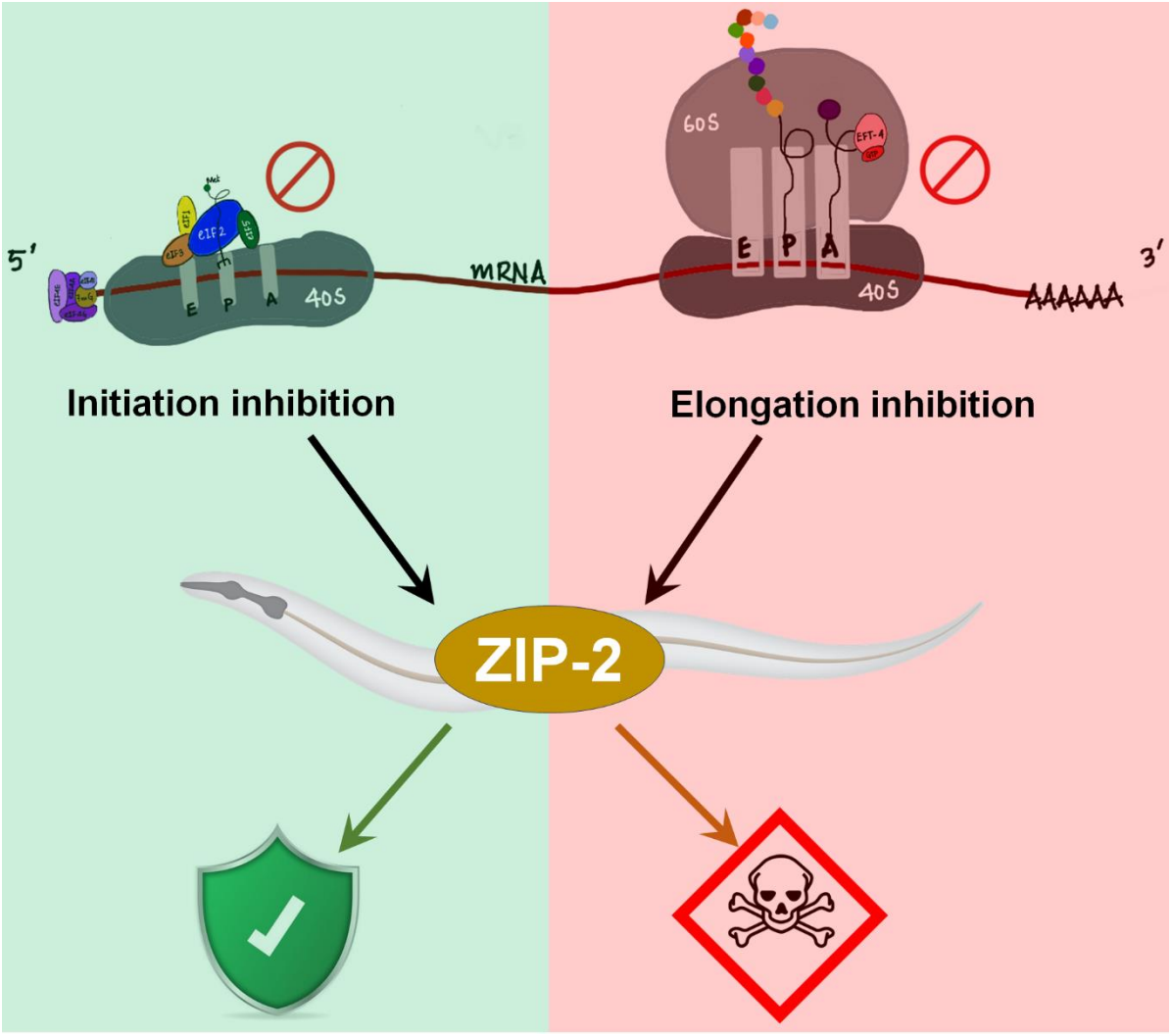

Figure 6. Model for the impact of translation inhibition on *C. elegans* survival on *P. aeruginosa*

Inhibition of several translation initiation factors improves *C. elegans* survival on *P. aeruginosa* via ZIP-2-mediated immune responses. Conversely, inhibition of elongation factors decreases the survival of *C. elegans* on *P. aeruginosa*, which is also executed by ZIP-2.

Supplementary Figures

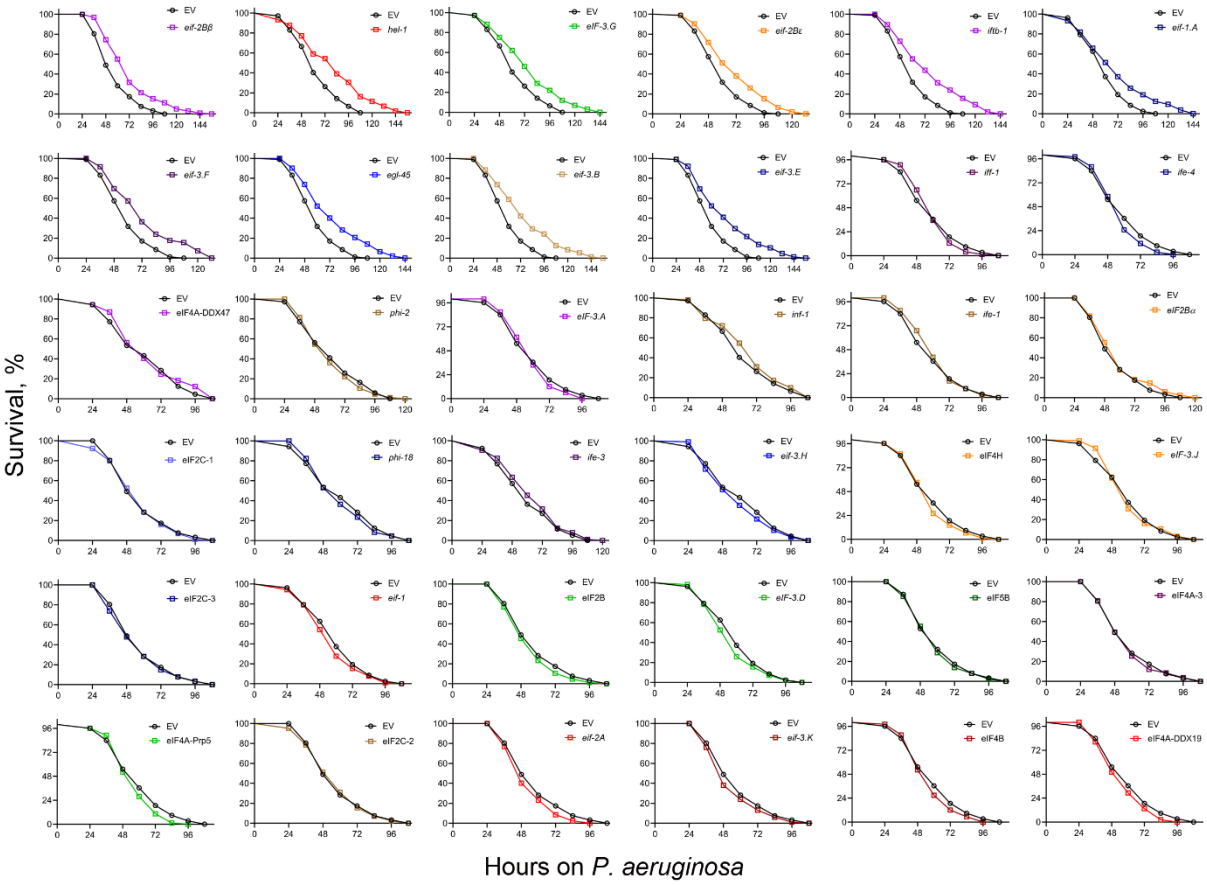

Figure S1. Inhibition of several translation initiation factors improves *C. elegans* survival on *P. aeruginosa*

Representative survival plots of N2 animals on *P. aeruginosa* PA14 at 25°C after treatment with the empty vector (EV) control and RNAi against various translation initiation factors. The EV control is common for different cohorts of the survival curves. Detailed statistical analysis is available in Table S2.

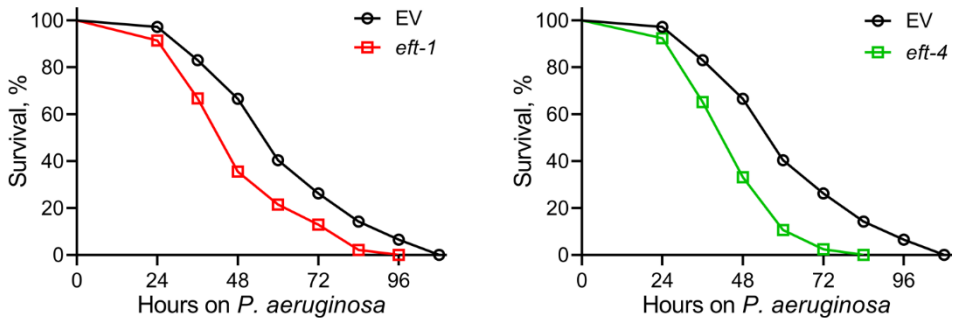

Figure S2. Inhibition of translation elongation factors reduces *C. elegans* survival on *P. aeruginosa*

Representative survival plots of N2 animals on *P. aeruginosa* PA14 at 25°C after treatment with the empty vector (EV) control, *eft-1*, and *eft-4* RNAi. The EV control is common for the two survival plots. Detailed statistical analysis is available in Table S2.

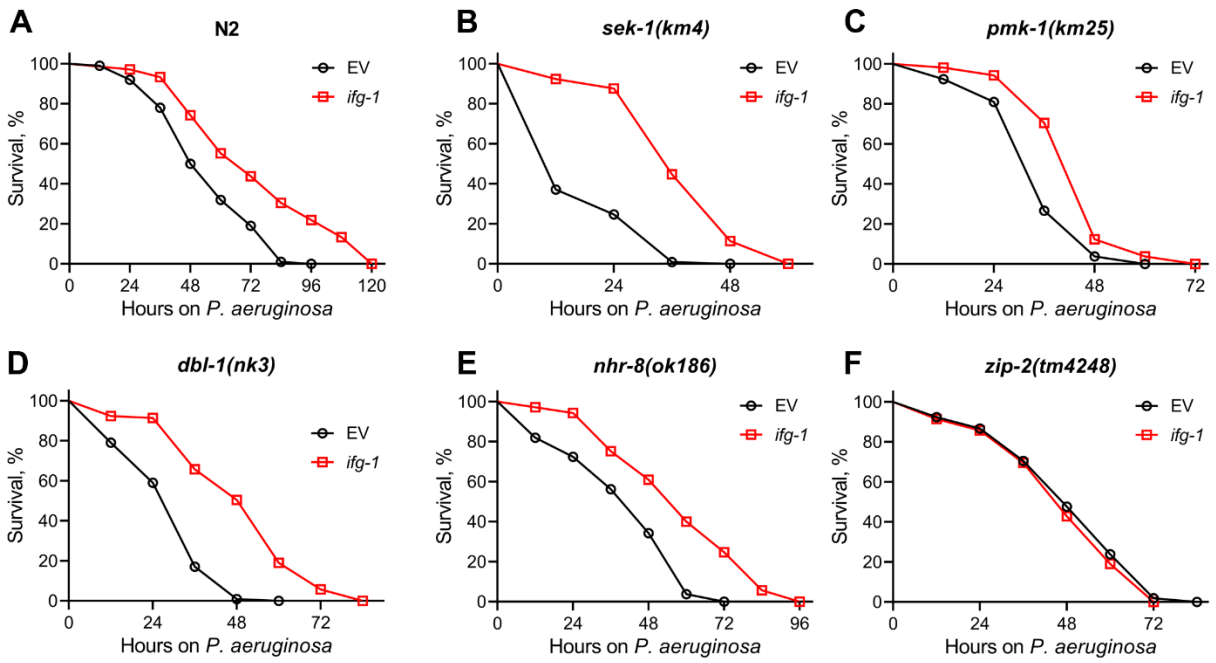

Figure S3. Knockdown of *ifg-1* increases *C. elegans* survival on *P. aeruginosa* via transcription factor ZIP-2

Representative survival plots of N2 (A), *sek-1(km4)* (B), *pmk-1(km25)* (C), *dbl-1(nk3)* (D), *nhr-8(ok186)* (E), and *zip-2(tm4248)* (F) animals on *P. aeruginosa* PA14 at 25°C after treatment with the empty vector (EV) control and *ifg-1* RNAi. $P<0.001$ for *ifg-1* RNAi compared to EV control for N2, *sek-1(km4)*, *pmk-1(km25)*, *dbl-1(nk3)*, and *nhr-8(ok186)* animals. Survival curves for *ifg-1* RNAi compared to the EV control for *zip-2(tm4248)* animals are nonsignificant.

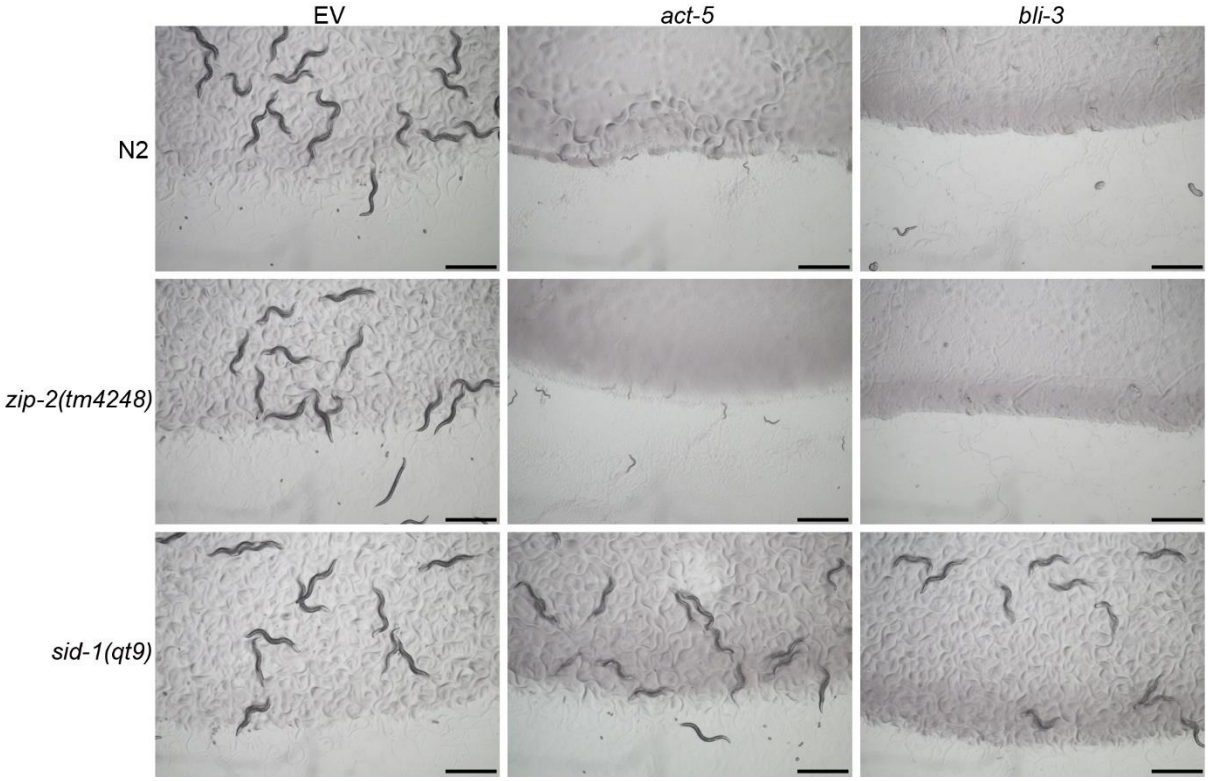

Figure S4. The *zip-2(tm4248)* animals are sensitive to RNAi

Representative images of wild-type N2, *zip-2(tm4248)*, and *sid-1(qt9)* worms on the empty vector (EV) control, *act-5*, and *bli-3* RNAi. Scale bar = 1 mm.

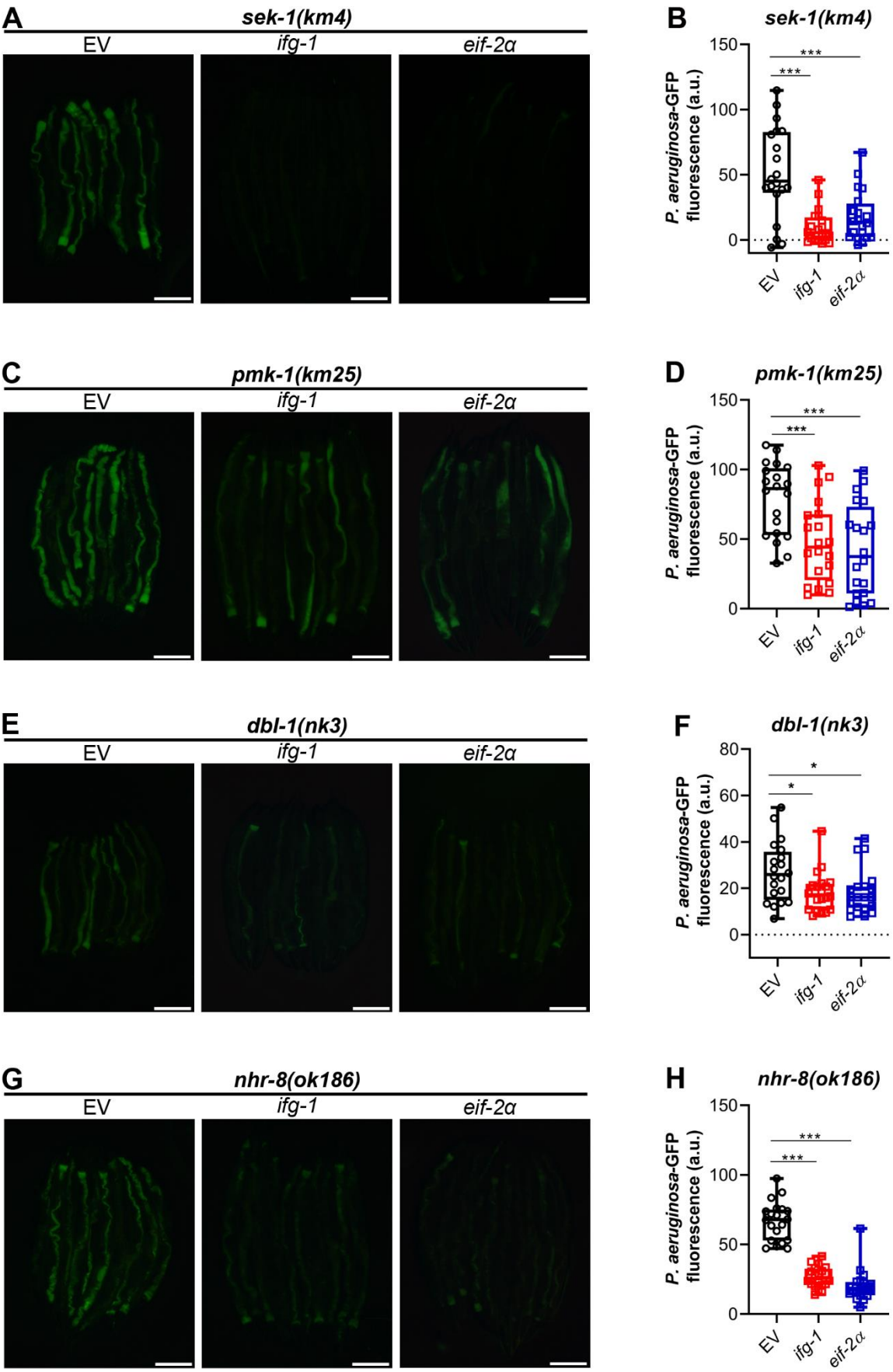

Figure S5. Inhibition of *eif-2α* and *ifg-1* results in reduced *P. aeruginosa* colonization in

***sek-1(km4), pmk-1(km25), dbl-1(nk3),* and *nhr-8(ok186)* animals**

(A) Representative fluorescence images of *sek-1(km4)* animals incubated on *P. aeruginosa*-GFP for 12 hours at 25°C after treatment with the empty vector (EV) control, *ifg-1*, and *eif-2α* RNAi. Scale bar = 200 μm.

(B) Quantification of GFP levels of *sek-1(km4)* animals incubated on *P. aeruginosa*-GFP for 12 hours at 25°C after treatment with the EV control, *ifg-1*, and *eif-2α* RNAi. ***$P < 0.001$ and via the *t*-test ($n = 20$ worms each).

(C) Representative fluorescence images of *pmk-1(km25)* animals incubated on *P. aeruginosa*-GFP for 24 hours at 25°C after treatment with the EV control, *ifg-1*, and *eif-2α* RNAi. Scale bar = 200 μm.

(D) Quantification of GFP levels of *pmk-1(km25)* animals incubated on *P. aeruginosa*-GFP for 24 hours at 25°C after treatment with the EV control, *ifg-1*, and *eif-2α* RNAi. ***$P < 0.001$ via the *t*-test ($n = 20$ worms each).

(E) Representative fluorescence images of *dbl-1(nk3)* animals incubated on *P. aeruginosa*-GFP for 24 hours at 25°C after treatment with the EV control, *ifg-1*, and *eif-2α* RNAi. Scale bar = 200 μm.

(F) Quantification of GFP levels of *dbl-1(nk3)* animals incubated on *P. aeruginosa*-GFP for 24 hours at 25°C after treatment with the EV control, *ifg-1*, and *eif-2α* RNAi. *$P < 0.05$ via the *t*-test ($n = 20$ worms each).

(G) Representative fluorescence images of *nhr-8(ok186)* animals incubated on *P. aeruginosa*-GFP for 24 hours at 25°C after treatment with the EV control, *ifg-1*, and *eif-2α* RNAi. Scale bar = 200 μm.

(H) Quantification of GFP levels of *nhr-8(ok186)* animals incubated on *P. aeruginosa*-GFP for 24 hours at 25°C after treatment with the EV control, *ifg-1*, and *eif-2α* RNAi. ***$P < 0.001$ via the *t*-test ($n = 20$ worms each).

Table S1: The list of *C. elegans* translation factors available in the Ahringer RNAi library and the effects of their knockdown on the development and fertility of N2 wild-type worms

Initiation factors		
Predicted translation factors	**Gene ID**	**Development/fertility**
eif-1	T27F7.3	L4
eif-1.A	H06H21.3	Late L4/young adults
eif-2A	E04D5.1	Adults
eif-2α	Y37E3.10	L3-L4
iftb-1	K04G2.1	L3
eIF2B	C01G10.9	Adults
eif-2Bα	ZK1098.4	Adults
eif-2Bβ	Y47H9C.7	Adults
eif-2Bε	D2085.3	L4
eif-2Bγ	C15F1.4	Adults (sterile)
eIF2C-1	T22B3.2	Adults
eIF2C-2	ZK757.3	Adults
eIF2C-3	R09A1.1	Adults
egl-45	C27D11.1	L4
eif-3.A	F55H2.6	Adults
eif-3.B	Y54E2A.11	L3
eif-3.C	T23D8.4	Late L4/young adults
eif-3.D	R08D7.3	L3
eif-3.E	B0511.10	L4
eif-3.F	D2013.7	L3
eif-3.G	F22B5.2	L3
eif-3.H	C41D11.2	Late L4/Adults
eif-3.J	Y40B1B.5	L4
eif-3.K	T16G1.11	Adults
inf-1	F57B9.6	L3
phi-2	F57B9.3	L4
eIF4A-3	F33D11.10	Adults
eIF4A-p56	C07H6.5	Adults (sterile)
hel-1	C26D10.2	L4
eIF4A-DDX47	T26G10.1	L4
eIF4A-DDX19	T07D4.4	Adults
eIF4A-Prp5	F53H1.1	Adults
eIF4B	Y73B6BL.33	Adults
ife-1	F53A2.6	Adults
ife-2	R04A9.4	Adults
ife-3	B0348.6	Adults
ife-4	C05D9.5	Adults
ifg-1	M110.4	L3
eIF4H	T12D8.2	Adults

phi-18	C37C3.2	L4
iff-1	T05G5.10	Adults
iff-2	F54C9.1	Adults (sterile)
eIF5B	Y54F10BM.2	Adults
Elongation factors		
Predicted translation factors	**Gene ID**	**Development/fertility**
eft-4	R03G5.1	L3-L4
eef-1B.2	Y41E3.10	Adults
eft-2	F25H5.4	L3
eft-1	ZK328.2	L3

Table S2: Statistical analysis of survival curves from three independent experiments for each condition. A separate Excel file is provided.

Table S3: Quantitative reverse transcription-PCR primers used in the study

Gene name	Forward primer sequence (5'-3')	Reverse primer sequence (5’-3’)
Pan-act	TCGGTATGGGACAGAAGGAC	CATCCCAGTTGGTGACGATA
irg-1	TCCGAAGACCGCACAAAAGT	TTTAGCCTCAAAGCCGGAGG
irg-2	ACTCAATTCGTGGCCAACCT	TGCCCAGTAACTTGTGTGGG
ugt-31	TCCCCAGACGGCTCTTCTAA	ACATCGGAGCATTACGTCCC
T16G1.5	GAATGACGCGCTGTTGAGTC	TTGGATGCAACTCGTGTGGT
Y51B9A.8	AATCACCTGTAACGGAGGGC	TGCAGCAATCACGAGCAGTA
cyp-14A5	ATCTTCTGCAGTTCCCAGCC	CTGCAGGTAGTGGTGTCCAG
oac-32	TGGAACCTGTCTTGGACTTTCC	TGTCCACGGAGACAAAAGCA
pgp-5	CCCTTGTTGCCATTTTCAAGC	CAAACGGTTGACACATACCAGT
E02C12.8	TGTCAAGAATCGCCTGCCTT	GCTGAGAGCTTATCTTCAACGC